

## Nonthermal phenomena in clusters of galaxies

Y. Rephaeli · J. Nevalainen · T. Ohashi ·  
A.M. Bykov

Received: 1 October 2007; Accepted: 5 December 2007

**Abstract** Recent observations of high energy ( $> 20$  keV) X-ray emission in a few clusters of galaxies broaden our knowledge of physical phenomena in the intracluster space. This emission is likely to be nonthermal, probably resulting from Compton scattering of relativistic electrons by the cosmic microwave background (CMB) radiation. Direct evidence for the presence of relativistic electrons in some 50 clusters comes from measurements of extended radio emission in their central regions. We briefly review the main results from observations of extended regions of radio emission, and Faraday rotation measurements of background and cluster radio sources. The main focus of the review are searches for nonthermal X-ray emission conducted with past and currently operating satellites, which yielded appreciable evidence for nonthermal emission components in the spectra of a few clusters. This evidence is clearly not unequivocal, due to substantial observational and systematic uncertainties, in addition to virtually complete lack of spatial information. If indeed the emission has its origin in Compton scattering of relativistic electrons by the CMB, then the mean magnetic field strength and density of relativistic electrons in the cluster can be directly determined. Knowledge of these basic nonthermal quantities is valuable for the detailed description of processes in intracluster gas and for the origin of magnetic fields.

**Keywords** Clusters: general, X-ray emission

---

Y. Rephaeli  
School of Physics & Astronomy, Tel Aviv University, Tel Aviv, 69978, Israel  
Center for Astrophysics and Space Sciences, University of California, San Diego, La Jolla,  
CA 92093-0424  
E-mail: yoelr@wise.tau.ac.il

J. Nevalainen  
Observatory, P.O. Box 14, 00014 University of Helsinki, Helsinki, Finland

T. Ohashi  
Department of Physics, Tokyo Metropolitan University, 1-1 Minami-Osawa, Tokyo 192-0397,  
Japan

A.M. Bykov  
A.F. Ioffe Institute for Physics and Technology, 194021 St. Petersburg, Russia

## 1 Introduction

Clusters of galaxies are the largest bound systems and the most important link to the large scale structure (LSS) of the Universe. The detailed properties of clusters, such as the distributions of their various mass constituents - dark matter, hot intracluster (IC) gas, and galaxies - dynamics, and thermal structure, are of much interest both intrinsically, and for the understanding of the formation and evolution of the LSS. Moreover, detailed *astrophysical* knowledge of clusters is essential for their use as *precise* cosmological probes to measure global parameters, such as  $H_0$ ,  $\Omega_M$ , &  $\Omega_A$ , and parameters characterising the primordial density fluctuation field.

Recent observations of many clusters of galaxies with the *Chandra* and *XMM* satellites at energies  $\epsilon \leq 10$  keV, have significantly advanced our knowledge of the morphology and thermal structure of hot IC gas, the source of the cluster thermal Bremsstrahlung emission. The improved determinations of the gas temperature, density, and metal abundances from these observations significantly improve estimates of such important quantities as the total cluster mass and its gaseous and baryonic mass fractions.

As has been the case in galaxies, in clusters too a more physically complete understanding of these systems necessitates knowledge also of non-thermal (NT) quantities and phenomena in the IC space. Observational evidence for the relevance of these phenomena in clusters comes mostly from measurements of extended regions of radio emission, and from Faraday rotation (FR) of the plane of polarisation of radio sources seen through (or inside) clusters. Since the observed radio emission is clearly synchrotron-produced, its level and spectrum yield direct information on IC relativistic electrons and magnetic fields. Information on cluster magnetic fields (separately from relativistic electron properties) is obtained also from FR measurements. Compton scattering of cosmic microwave background (CMB) photons by the radio-emitting relativistic electrons boosts photon energies to the X-and- $\gamma$  regions (e.g., Rephaeli 1979). The search for cluster NT X-ray emission has begun long ago (Rephaeli et al. 1987), but first clear indications for emission at energies  $\epsilon \geq 20$  keV came only after deep dedicated observations of a few clusters with the *RXTE* and *BeppoSAX* satellites (beginning with analyses of observations of the Coma cluster (Rephaeli et al. 1999; Fusco-Femiano et al. 1999). Radio and NT X-ray observations provide quantitative measures of very appreciable magnetic fields and relativistic electron densities in the observed clusters. These results open a new dimension in the study of clusters.

This is a review of cluster NT X-ray observations and their direct implications, including prospects for the detection of  $\gamma$ -ray emission. The literature on cluster NT phenomena is (perhaps somewhat surprisingly) quite extensive, including several reviews of radio emission (e.g., Govoni & Feretti 2004) and cluster magnetic fields (e.g., Carilli & Taylor 2002), and a review of the current status of radio observations by Ferrari et al. 2008 - Chapter 6, this volume. In order to properly address the comparison between magnetic field values deduced from radio observations and jointly from NT X-ray and radio measurements, we include here a brief summary of cluster radio observations. Measurements of EUV emission in a few clusters, and claims that this emission is by energetic electrons, are reviewed by Durret et al. 2008 - Chapter 4, this volume. NT radiation processes are reviewed by Petrosian et al. 2008 - Chapter 10, this volume, and relevant aspects of particle acceleration mechanisms are reviewed by Petrosian & Bykov 2008 - Chapter 11, this volume.

---

## 2 Radio Observations

Measurements of synchrotron radio emission at several frequencies usually provide the first evidence for the presence of a significant population of relativistic electrons and magnetic fields. This has been the prime evidence for IC fields and electrons. In addition, Faraday Rotation (FR) of the plane of polarisation of radiation from cluster and background radio galaxies has provided mostly statistical evidence for IC magnetic fields. Main results from these very different sets of observations are briefly reviewed in the next two subsections.

### 2.1 Extended IC Emission

In clusters the task of actually determining that the observed emission is from extended IC regions is quite challenging, since high resolution observations of the various discrete radio sources (that are mostly in the member galaxies) are required, in addition to the (lower resolution) observations of the extended low brightness emission. The truly extended emission is mapped upon subtraction of the respective contributions of these sources to the spectral flux. Observations of extended radio emission had begun some 50 years ago with measurements of Coma C in the central region of the Coma cluster by Seeger et al. (1957), followed by various other measurements at frequencies in the range 0.01 – 4.85 GHz, including the first detailed study at 408 MHz and 1407 MHz by Willson (1970).

Appreciable effort has been devoted to measure extended emission regions in clusters, which has resulted in the mapping of centrally located (‘halo’) and other (‘relic’) regions in about 50 clusters. Some 32 of these were found in a VLA survey (Giovannini et al. 1999; Giovannini & Feretti 2000) of 205 nearby clusters in the ACO catalogue, only about a dozen of these were previously known to have regions of extended radio emission. Primary interest (certainly to us here) is in the former sources, which constitute a truly cluster phenomenon. A central extended radio region (which is somewhat inappropriately referred to as ‘halo’) typically has a size of  $\sim 1 - 2$  Mpc, and a luminosity in the range  $10^{40} - 10^{42}$  ergs $^{-1}$  (for  $H_0 = 70$  km s $^{-1}$  Mpc $^{-1}$ ) over the frequency band  $\sim 0.04 - 5$  GHz. With radio indices usually in the range  $\sim 1 - 2$ , the emission is appreciably steeper than that of (most) radio galaxies.

The clusters in which radio halos and relics have already been found include evolving systems with a substantial degree of subclustering, as well as well-relaxed clusters that seem to have attained hydrostatic equilibrium. Halo morphologies are also quite varied, from roughly circular (projected) configuration to highly irregular shape, as can be seen in the contour maps produced by Giovannini et al. (1999); Giovannini & Feretti (2000); Giovannini et al. (2006). The spatial variety is reflected also in the wide distribution of values of the spectral index across the halo; e.g. see the maps in Giovannini et al. (1999).

Obviously, the magnetic field strength and relativistic electron density cannot both be determined from radio measurements alone, unless it is assumed that they are related so both can be determined from a single observable. It is commonly assumed that the total energy density of particles (mostly, protons and electrons) is equal to that in the magnetic field. The validity of this equipartition assumption is not obvious, especially in clusters where the particles and fields may have different origins and evolutionary histories. Moreover, the complex nature of the radio emission, and

the expected significant variation of the magnetic field strength and relativistic electron density across a halo, imply that only rough estimates of these quantities can be obtained from measurements of the (spectral) flux integrated over the halo. When available, values of the halo mean equipartition field,  $B_{\text{eq}}$ , are also listed in Table 1; generally, these substantially uncertain values are at the few  $\mu\text{G}$  level.

## 2.2 Faraday Rotation

IC magnetic fields can also be estimated by measuring the statistical depolarisation and Faraday Rotation of the plane of polarisation of radiation from background radio sources seen through clusters (e.g. Kim et al. 1991), and also from radio sources in the cluster. FR measurements sample the line of sight component of the randomly oriented (and spatially dependent) IC fields, weighted by the gas density, yielding a mean weighted value which we denote by  $B_{\text{fr}}$ . This quantity was estimated by analysing the rotation measure (RM) distribution of individual radio sources in several clusters, including Cygnus A (Dreher et al. 1987), Hydra A (Taylor & Perley 1993; Vogt & Enßlin 2003), A 119 (Feretti et al. 1999; Dolag et al. 2001), A 400, and A 2634 (Vogt & Enßlin 2003). Analyses of FR measurements typically yield values of  $B_{\text{fr}}$  that are in the range of  $1 - 10 \mu\text{G}$ .

Most FR studies are statistical, based on measurements of radio sources that are inside or behind clusters. An example is the work of Clarke et al. (2001), who determined the distribution of RM values with cluster-centric distance for 27 radio sources within or in the background (15 and 12, respectively) of 16 nearby clusters. Analysis of this distribution (including comparison with results for a control sample of radio sources seen outside the central regions of the clusters in the sample) yielded a mean field value of  $\sim 5 - 10 (\ell/10 \text{ kpc})^{-1/2} \mu\text{G}$ , where  $\ell$  is a characteristic field spatial coherence (reversal) scale. In further work the sample of radio sources was significantly expanded (to about 70; Clarke 2004). In comparing different measures of the mean strength of IC fields it should be remembered that the selective sampling of locally enhanced fields in high gas density regions in cluster cores broadens the RM distribution, resulting in overestimation of the field mean strength.

Deduced values of  $B_{\text{fr}}$  yield substantially uncertain estimates of the mean field across a halo. The major inherent uncertainties stem from the need to separate the several contributions to the total RM (including that which is intrinsic to the radio source), the unknown tangled morphology of IC fields and their spatial variation across the cluster, as well as uncertainty in modelling the gas density profile. A discussion of these uncertainties, many aspects of which have already been assessed in some detail (e.g., Goldshmidt & Rephaeli 1993; Newman et al. 2002; Rudnick & Blundell 2003; Enßlin et al. 2003; Murgia et al. 2004), is out of the scope of our review.

## 3 Nonthermal X-ray Emission

As has been noted long ago, Compton scattering of the CMB by relativistic electrons boosts photon energies to the X-ray and  $\gamma$ -ray regions. Measurement of this radiation provides additional information that enables the determination of the electron density and mean magnetic field directly, *without* the need to invoke equipartition. The mean strength of the magnetic field which is deduced from the radio and NT X-ray fluxes,

$B_{rx}$ , is essentially a volume average over the emitting region. The detection of IC radio and NT X-ray emission sets the stage for a more meaningful study of the origin of magnetic fields and cosmic rays in extragalactic environments.

The focus of this review are measurements of NT X-ray emission in large extended IC regions. NT emission is obviously predicted within dominant radio galaxies in the centres of clusters and in their radio halos. This emission has been sought in several galaxies including NGC 1275 in the Perseus cluster (e.g., Sanders & Fabian 2003) and M 87 in Virgo (Simionescu et al. 2007), but does not seem to have been detected. The mapping of the electron spectrum in these inner regions clearly provides crucial information on the initial source of IC relativistic electrons and most likely also energetic protons, whose energy input and heating of the gas could possibly be important in the inner core of Perseus (Rephaeli & Silk 1995) and other clusters. NT X-ray emission in these environments is quite complex due to its multi-source (AGN, jet, binaries, and halo), temporally variable nature. A discussion of NT emission in these essentially galactic environments is out of the scope of our review.

The prospects for measuring cluster NT X-ray emission motivated detailed calculations of the predicted emission (Rephaeli 1977, 1979). In these calculations the relativistic electron spectrum was directly related to the measured radio spectrum and no attempt was made to model the spectra of possible energetic electron populations. Energetic protons, which are a major Galactic cosmic ray component, are also expected in the IC space, particularly so in the inner cores of clusters dominated by a radio galaxy. Their interactions with protons in the gas produce neutral and charged pions, whose decays yield  $\gamma$ -ray emission and secondary electrons (e.g., Dennison 1980; Dermer & Rephaeli 1988; Blasi & Colafrancesco 1999). Energetic protons also deposit energy and heat IC gas through their Coulomb interactions with electrons and protons in the gas (Rephaeli 1987; Rephaeli & Silk 1995).

With mean field values in the range of  $0.1 - 1 \mu\text{G}$ , the energy range of electrons emitting at the observed radio frequencies is  $\sim 1 - 100 \text{ GeV}$ . Of course, electrons with energies outside this range are also expected, either as part of the same or a different population. In particular, NT Bremsstrahlung EUV and X-ray emission by (the more numerous) lower energy electrons would also be expected (Kaastra et al. 1998; Sarazin 1999). However, at energies below  $\sim 200 \text{ MeV}$ , the main energy loss is electronic excitations in the gas (Rephaeli 1979); this sets a stringent limit on the contribution to the NT X-ray emission by a low energy electron population (Rephaeli 2001; Petrosian 2001). We will therefore assume that NT X-ray emission is largely due to Compton scattering of radio-emitting electrons by the CMB.

The main characteristics of the predicted Compton-produced emission are: (a) X-ray to radio flux ratio is roughly equal to the ratio of the CMB energy density to the magnetic field energy density. (b) Power-law index is nearly equal to the radio index. (c) Matching X-ray and radio centroids, with the X-ray spatial profile generally shallower than that of the radio emission. These features are expected only if the Compton-produced emission is identified and separated from other contributions, the primary thermal emission as well as NT emission from relics and individual galaxies. Due to source confusion, as well as other systematic and observational uncertainties, spatial information is *crucially* needed in order to clearly identify the origin of NT X-ray emission.

We first briefly summarise the required sensitivity and level of spatial resolution for the detection of NT emission, and then review the results of the search for this emission with the *HEAO-1*, *CGRO*, *RXTE*, *BeppoSAX*, *Suzaku*, and *INTEGRAL*.

### 3.1 Instrumental Requirements

Cluster X-ray emission is primarily thermal up to  $\sim 30 - 40$  keV; therefore, clear identification of NT emission necessitates also precise measurement of the thermal emission in order to account for and separate it from the sought NT component. The required detector spectral range must therefore extend down to sufficiently low energies.

Using standard expressions for Compton and synchrotron emission from the same population of relativistic electrons, the predicted level of Compton-produced emission from nearby clusters with measured radio halos can be readily estimated. Since imaging information at the high energy X-ray regime ( $\epsilon > 30$ ) is minimal at best, we will ignore spatial factors in the Compton-synchrotron formulae (e.g., Rephaeli 1979) that include integrals over the relativistic electron and magnetic fields spatial profiles. This is valid as long as the NT X-ray emission region coincides with the radio region. We base our estimate of the required detector sensitivity on the level of radio emission as measured in the nearby clusters with well measured halos (such as Coma, A 2256, A 2319), for which the feasibility of detection of the NT emission is likely to be highest. Using the range of values for radio spectral index and flux, we estimate the level of NT flux at 40 keV to be typically  $\sim 1 \times 10^{-6} \text{ cm}^{-2} \text{ s}^{-1} \text{ keV}^{-1}$  and an integrated flux of  $\sim 3 \times 10^{-5} \text{ cm}^{-2} \text{ s}^{-1}$  in the 40 – 80 keV band, if the mean field (across the emitting region) is  $B \sim 0.3 \mu\text{G}$ . The value of the field is critical due to the strong  $B$  dependence of the flux, with a power-law exponent typically larger than 2. For example, the predicted flux in the Coma cluster is some 16 times lower if  $B = 1 \mu\text{G}$ .

Given the great difficulty in detecting the predicted NT flux at energies  $\epsilon \geq 40$  keV, it is only reasonable to search for it also at lower energies. To do so optimally would require a high-sensitivity detector that covers a wider spectral band than that of any previously flown instrument. Combining measurements made with two different detectors is problematic, given the inherent difficulty in the requisite precise cross-calibration (at the  $\sim 1\%$  level) of signals from detectors on the same satellite, and even more so when the detectors were on different satellites altogether. An added difficulty arises in the extremely difficult task of detecting a weak secondary component at energies below  $\sim 1$  keV where photoelectric absorption is strong. This should be kept in mind when assessing results from such combined analyses, some of which are discussed below.

Even if NT emission is detected its origin has to be verified before it is identified with electrons in the halo. The first requirement is that the measured emission does not show any temporal variation (that would usually imply AGN origin). Sizes of radio halos in nearby clusters are in the range of  $15' - 30'$ , which in principle can be resolved by the *IBIS* instrument aboard *INTEGRAL*, the first imaging experiment in the high energy X-ray regime. Clearly, higher detector sensitivity is required for resolved measurements of such large regions. All the other presently active (and previous) satellites with high energy spectral capability have FOVs that are larger than the halos of (even) nearby clusters. Measurements of NT emission have so far been solely spectral, thus providing only the necessary - but not sufficient - evidence for the detection of NT emission in a few clusters.

### 3.2 Initial search for NT X-ray emission

Systematic searches for NT X-ray emission began with the analysis of archival *HEAO-1* measurements of six clusters (Coma, A 401, A 2142, A 2255, A 2256, A 2319) with measured radio halos (Rephaeli et al. 1987; Rephaeli & Gruber 1988), and continued with *CGRO* observation of the Coma cluster (Rephaeli et al. 1994). No significant NT emission was detected, resulting in lower limits on the mean, volume-averaged magnetic fields in these clusters,  $B_{\text{rx}} = O(0.1 \mu\text{G})$ .

Observation of the Coma cluster with the *CGRO/OSSE* experiment for  $\sim 380$  ks was the first dedicated measurement of a cluster aimed at measuring NT emission. The fact that the predicted emission was not detected clearly established that instruments with higher detector sensitivity, significantly lower level of internal background, and much smaller FOV (than that of *OSSE*,  $\sim 1^\circ \times 1^\circ$  FWHM), are the minimal requirements for measurement of emission in the 40 – 100 keV band.

Attempts to measure NT emission from clusters continued with all subsequent X-ray satellites whose nominal spectral band extended beyond 10 keV. First observational evidence for NT emission came from long measurements with the *RXTE* and *BeppoSAX* satellites, as discussed in the next two subsections, followed by a review of results from *ASCA*, initial results from *Suzaku/HXD*, and the first spatial analysis of *INTEGRAL/IBIS* observations of the Coma cluster.

### 3.3 Search for NT emission with *RXTE*

The search for cluster NT emission advanced significantly through long observations with the PCA and HEXTE experiments aboard the *RXTE* satellite. These instruments have the minimally required capabilities for detection of a weak NT spectral component - sufficiently high sensitivity for precise measurement of the primary thermal emission, and good background subtraction achieved by (on and off source) ‘rocking’ of the HEXTE detectors. The crucial *RXTE* features which are essential for identifying the small NT component are spectral overlap of the two experiments over the effective (narrower than nominal)  $\sim 13 - 25$  keV band, and the same triangular spatial response function with  $58'$  FWHM. As has been noted already, the *RXTE* does not have the capability to resolve the emission even in nearby (rich) clusters, implying that the exact origin of NT emission cannot be identified even when a secondary spectral component is clearly detected.

We review here results of searches for NT components in the spectra of clusters that were observed for at least  $\sim 100$  ks. Shorter observations were mostly aimed at measurement of the primary thermal emission, with the exception of a 70 ks observation of A 754 (Valinia et al. 1999), and even shorter  $\sim 30$  ks observations of A 2256 (Henriksen 1999) and A 1367 (Henriksen & Mushotzky 2001), which resulted in upper limits on NT emission in these clusters. For obvious reasons, Coma was the first cluster searched for NT emission with *RXTE* (Rephaeli et al. 1999). The search continued with long observations of A 2319, A 2256, and A 2163, all with observed radio halos. Results of the search for NT emission in these and other clusters are listed in Table 1, and briefly described below.

**Coma:** The cluster was initially observed (in 1996) for  $\sim 90$  ks with the PCA, and for  $\sim 29$  ks with HEXTE. Analysis of these measurements showed evidence for the presence of a second spectral component at energies up to  $\sim 20$  keV (Rephaeli et al. 1999), but

**Table 1** NT emission parameters from *RXTE* measurements and (deduced mean radio-and-X-determined field)  $B_{\text{rx}}$ 

Cluster	20 – 80 keV flux ( $10^{-12}$ erg s $^{-1}$ cm $^{-2}$ )	$\Gamma$	$B_{\text{rx}}$ ( $\mu\text{G}$ )	Reference
Coma	$21 \pm 6$	$2.1 \pm 0.5$	0.1 – 0.3	Rephaeli & Gruber (2002)
A 2163	$11^{+17}_{-9}$	$1.8^{+0.9}_{-4.2}$	$0.4 \pm 0.2$	Rephaeli et al. (2006)
A 2256	$4.6 \pm 2.4$	$2.2^{+0.9}_{-0.3}$	$0.2^{+1.0}_{-0.1}$	Rephaeli & Gruber (2003)
A 2319	$14 \pm 3$	$2.4 \pm 0.3$	0.1 – 0.3	Gruber & Rephaeli (2002)
A 3667	$\leq 4$	$\sim 2.1$	$\geq 0.4$	Rephaeli & Gruber (2004)
1ES 0657-55.8	$\sim 5 \pm 3$	$1.6 \pm 0.3$	1.2 <sup>a</sup>	Petrosian et al. (2006)

All quoted errors are at the 90 % confidence level.

<sup>a</sup> The magnetic field value in 1ES 0657-558 was derived assuming energy equipartition between the field and particles.

the nature of the secondary emission could not be determined. In order to improve the quality of the spectral results, the cluster was observed again (in 2000) for  $\sim 177$  ks. Analysis of the new observations (Rephaeli & Gruber 2002, hereafter RG02) yielded results that are consistent with those from the first observation. Joint analysis of the full *RXTE* dataset shows that - from a statistical point of view - no preference could be determined for the nature of the secondary component. If thermal, the most probable temperature would be very high,  $kT_2 \simeq 37.1$  keV, but at its lowest boundary, the 90 % contour region includes a much lower, physically more acceptable value. However, the best fit combination of the temperatures of the primary and secondary components is then  $kT_1 = 5.5$  keV, and  $kT_2 = 9$  keV, respectively, with the respective 4 – 20 keV fractional fluxes of  $\sim 24$  % and  $\sim 76$  %. RG02 argued that it is quite unlikely that about a quarter of the emission comes from gas at a significantly lower temperature than the mean value deduced by virtually all previous X-ray satellites. In particular, such a component would have been detected in the high spatially resolved *XMM* and *Chandra* maps of the cluster.

To quantitatively assess the possibility that a two-temperature gas model is just a simplified representation of a more realistic continuous temperature distribution, RG02 have assumed a polytropic gas temperature profile of the form  $T(r) \propto n(r)^{\gamma-1}$ , with a  $\beta$  profile for the gas density,  $n(r) \propto (1+r^2/r_c^2)^{-3\beta/2}$ , where  $r_c$  is the core radius. With these profiles they calculated the integrated flux and the mean emissivity-weighted temperatures as functions of  $\gamma$ ,  $\beta$ , and  $r$ . These quantities were then calculated in the projected (2D) circular regions  $[0, R]$  and  $[R, R_0]$  by convolving over the triangular response of the PCA with  $R_0 \simeq 58'$ . From ROSAT observations,  $r_c \sim 10.0'$ , and  $\beta \simeq 0.70 \pm 0.05$  (Mohr et al. 1999). The range of values of  $R$ ,  $\beta$ , and  $\gamma$  for which the two mean emissivity-weighted temperatures and respective fluxes from these regions were closest to the values deduced from the spectral analysis, were then determined. The results of these calculations indicate that for  $0.5 \leq \beta \leq 0.9$  and  $1 \leq \gamma \leq 5/3$ , there is no acceptable polytropic configuration that matches the observationally deduced values of the temperatures and fractional fluxes. For low values of  $\gamma$  the temperature gradient is too shallow, whereas for high  $\gamma$  values the implied central temperature is unrealistically high. Based on these results RG02 concluded that the two thermal components model does not seem to be consistent with the *RXTE* measurements, but certainly could not be ruled out.

Clearly, a search for NT emission motivated the long observation, and this alternative origin was assessed in detail by RG02. Since emission from an AGN in the



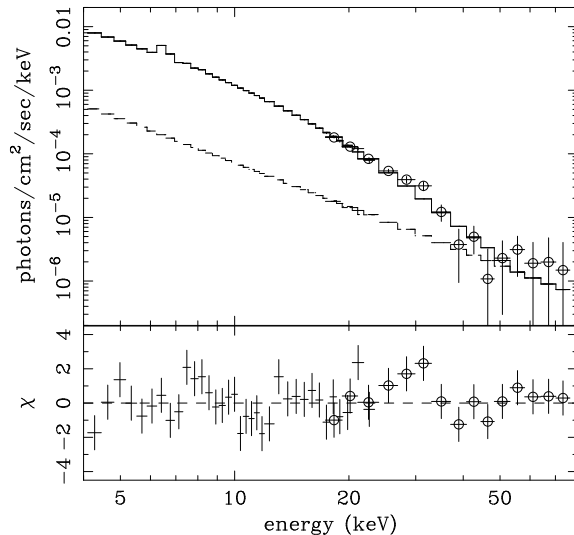


**Fig. 1** The RXTE spectrum of the Coma cluster and folded Raymond-Smith ( $kT \simeq 7.67$ ), and power-law (photon index = 2.3) models (from Rephaeli & Gruber 2002). HEXTE data points are marked with circles and 68 % error bars. The total fitted spectrum is shown with a histogram, while the lower histogram shows the power-law portion of the best fit. The quality of the fit is demonstrated in the lower panel, which displays the observed difference normalised to the standard error of the data point.

FOV was considered unlikely, they assessed whether the secondary emission is due to Compton scattering of relativistic electrons whose presence in Coma is directly inferred from many measurements of spatially extended region of radio emission (e.g. Kim et al. 1991; Giovannini et al. 1993; Thierbach et al. 2003). From the measured radio spectral index,  $1.34 \pm 0.1$ , it follows that the predicted power-law (photon) flux from Compton scattering of these electrons by the CMB should have an index  $\Gamma \sim 2.3$ . A power-law fit to the secondary component yielded  $2.1 \pm 0.5$  at the 90 % confidence level (CL). Results of this fit are shown in Fig. 1.

With the measured mean radio flux of  $0.72 \pm 0.21$  Jy at 1 GHz, and the deduced level of power-law X-ray flux, the mean volume-averaged value of the magnetic field,  $B_{\text{rx}}$ , was computed to be in the range  $0.1 - 0.3 \mu\text{G}$ . As noted by RG02, this estimate is based on the assumption that the spatial factors in the theoretical expressions for the two fluxes (Rephaeli 1979) are roughly equal, an implicit assumption made in virtually all previous attempts to derive the strength of cluster fields from radio and X-ray measurements.

A similar procedure was employed in analyses of observations of the other clusters (A 2319, A 2256, and A 2163) that were initiated by Rephaeli & Gruber.

**A 2319:** The cluster was observed (in 1999) for  $\sim 160$  ks. Analysis of the data (Gruber & Rephaeli 2002) showed no noticeable variability over the  $\sim 8$  week observation. The quality of the data allowed a meaningful search for emission whose spectral properties are distinct from those of the primary thermal emission with measured mean temperature in the range 8 – 10 keV. A fit to a single thermal component yielded  $kT = 8.6 \pm 0.1$  (90 % CL), a low iron abundance  $Z_{\text{Fe}} \sim 0.16 \pm 0.02$ , and large

positive residuals below 6 keV and between 15 to 30 keV. The quality of the fit was very significantly improved when a second component was added. A two-temperature model yielded  $kT_1 \simeq 10.1 \pm 0.6$ ,  $kT_2 \simeq 2.8 \pm 0.6$ , and  $Z_{\text{Fe}} \sim 0.23 \pm 0.03$ , a value consistent with previously measured values. An equally good fit was obtained by a combination of primary thermal and secondary NT components, with  $kT \simeq 8.9 \pm 0.6$ , and photon index  $\Gamma \simeq 2.4 \pm 0.3$ . Similar results were obtained when a joint analysis was performed of the *RXTE* data and archival *ASCA* data. The deduced value of  $\Gamma$  is consistent with the measured spectrum of extended radio emission in A2319. Identification of the power-law emission as Compton scattering of the radio-emitting electrons by the CMB resulted in  $B_{\text{rx}} \sim 0.1 - 0.3 \mu\text{G}$ , and  $\sim 4 \times 10^{-14} (R/2 \text{ Mpc})^{-3} \text{ erg cm}^{-3}$  for the mean energy density of the emitting electrons in the central region (radius  $R$ ) of the cluster.

**A 2256:** Following a very short  $\sim 30$  ks observation of A 2256 (in 1997) - which resulted in an upper limit on NT emission (Henriksen 1999) - the cluster was observed (in 2001 and 2002) for a total of  $\sim 343$  ks (*PCA*) and  $\sim 88$  ks (*HEXTE*). The data analysis (Rephaeli & Gruber 2003) yielded evidence for two components in the spectrum. Based on statistical likelihood alone the secondary component can be either thermal or power-law. Joint analysis of the *RXTE* and archival *ASCA* data sets yielded  $kT_1 = 7.9^{+0.5}_{-0.2}$  and  $kT_2 = 1.5^{+1.0}_{-0.4}$ , when the second component is also thermal, and  $kT = 7.7^{+0.3}_{-0.4}$  and  $\Gamma = 2.2^{+0.9}_{-0.3}$  (90 % CL), if the second component is a power-law. Identifying the secondary emission as due to Compton scattering of the radio producing relativistic electrons yielded  $B_{\text{rx}} \simeq 0.2^{+1.0}_{-0.1} \mu\text{G}$  in the central  $1^\circ$  region of the cluster, a region which contains both the halo and relic sources.

**A 2163:** The moderately-distant ( $z = 0.203$ ) cluster was observed for  $\sim 530$  ks (during a 6 month period in 2004). Primary thermal emission in this cluster comes from very hot IC gas with  $kT \sim 15$  keV, but analysis of the observations (Rephaeli et al. 2006) indicated very clearly that this component does not by itself provide the best fitting model. A secondary emission component was needed, and while this could also be thermal at a temperature significantly lower than 15 keV, the best fit to the full dataset was obtained with a power law secondary spectral component. The parameters of the NT emission imply a significant fractional flux amounting to  $\sim 25$  % of the integrated 3 – 50 keV emission. NT emission is expected given the intense level of radio emission, most prominently from a large radio halo. Rephaeli et al. (2006) assumed that the NT emission originates in Compton scattering of (the radio-emitting) relativistic electrons by the CMB, and estimated  $B_{\text{rx}} \sim 0.4 \pm 0.2 \mu\text{G}$  to be an overall mean field strength in the large complex region of radio emission in the cluster.

**A 3667:** The cluster was observed (in 2001 and 2002) for  $\sim 141$  ks; analysis of the *RXTE* observation and lower energy *ASCA* data, yielded only marginal evidence for a secondary power-law emission component in the spectrum (Rephaeli & Gruber 2004). This resulted in an upper limit of  $2.6 \times 10^{-12} \text{ erg cm}^{-2} \text{ s}^{-1}$  (at 90 % CL) on NT emission in the 15 – 35 keV band. When combined with the measured radio flux and spectral index of the dominant region of extended radio emission, this limit implies a lower limit of  $\sim 0.4 \mu\text{G}$  on the mean, volume-averaged magnetic field in A 3667.

**1ES 0657-55.8:** At  $z = 0.296$  the ‘bullet’ cluster is the most distant cluster searched for NT emission with *RXTE*. The cluster was observed (in 2002 and 2003) for a total of  $\sim 400$  ks. Joint analysis of the *RXTE* observations together with archival *XMM-Newton* observations clearly indicated the presence of a second spectral component (Petrosian et al. 2006). While the nature of this second component cannot be determined from the spectral analysis alone, the authors argue that a power-law spectral

shape is a more viable interpretation than an exponential. Since no radio data were available, the authors could only determine a mean field value of  $\sim 1.2 \mu\text{G}$  assuming energy equipartition between the field and relativistic electrons.

### 3.4 Search for NT emission with *BeppoSAX*

For observations of clusters the two relevant instruments were the MECS and PDS, the former with a spectral range of 1.3 – 10 keV,  $56'$  FOV and  $\sim 2'$  resolution, and the latter with response in the nominal 15 – 300 keV range and  $1.3^\circ$  FOV. The capability to separate the respective contributions of low and high energy components requires simultaneous and self-consistent measurements. For this reason the lack of spectral overlap of the two instruments (and their somewhat different FOV) was unfortunate.

#### 3.4.1 Observations of Individual Clusters

Results of searches for cluster hard X-ray emission are summarised in Table 2; a brief discussion of these results follows.

**Coma:** Fusco-Femiano et al. (1999) reported a  $4.5\sigma$  detection of excess emission above the primary thermal emission in  $\sim 91$  ks PDS observations carried out in 1997, but a later re-analysis resulted in a reduced estimate of the significance to  $3.4\sigma$  (Fusco-Femiano et al. 2004). The cluster was observed again for  $\sim 300$  ks (in 2000), and an analysis of the combined datasets - with a thermal component whose temperature was *assumed* to be  $kT = 8.1$  keV - yielded a  $4.8\sigma$  detection of excess emission in the 20 – 80 keV band (Fusco-Femiano et al. 2004). Assuming a power-law form for this excess emission with index  $\Gamma \sim 2.0$ , the 20-80 keV flux of  $1.5 \pm 0.5 \times 10^{-11}$  erg s $^{-1}$  cm $^{-2}$  was derived (a value which is consistent with that derived by Nevalainen et al. (2004). Interpreting this to be of Compton origin, and using the radio flux, resulted in  $B_{\text{rx}} \sim 0.2 \mu\text{G}$ .

Rossetti & Molendi (2004) questioned the reliability of the Fusco-Femiano et al. (1999, 2004) analyses. Having carried out their own analysis of 69 blank fields observed with PDS, they found that the two offset positions used for the local background determination yielded systematically different results for the background-subtracted flux. Since Fusco-Femiano et al. (1999, 2004) used only one offset pointing (due to contamination in the other offset field), without any adjustment for the systematic difference, Rossetti & Molendi (2004) claimed that the results of Fusco-Femiano et al. are incorrect. Based on the use of a different software package (SAXDAS) for background determination, Rossetti & Molendi (2004) determined that the significance of detection of excess emission in the original observation was only at the  $2\sigma$  level, while their analysis of the second observation yielded no evidence for excess emission, in strong contrast with the  $4.8\sigma$  detection level deduced by Fusco-Femiano et al. (2004).

The analysis was repeated (see Fig. 2) by Fusco-Femiano et al. (2007); they concluded that the discrepant results are due to the presence of two variable sources in one of the background fields, which is why they ignored that field in their analysis. The different background fields and the use of the XAS software (rather than SAXDAS) were suggested to be the reasons for the high significance ( $4.8\sigma$ ) detection reported by Fusco-Femiano et al. (2004). In a recent reply to Fusco-Femiano et al. (2007), Rossetti & Molendi (2007) defended their re-analysis and the lower detection significance of the hard excess, re-emphasising that the significance is highly sensitive to both the choice of the offset pointings for local background estimation, and also to

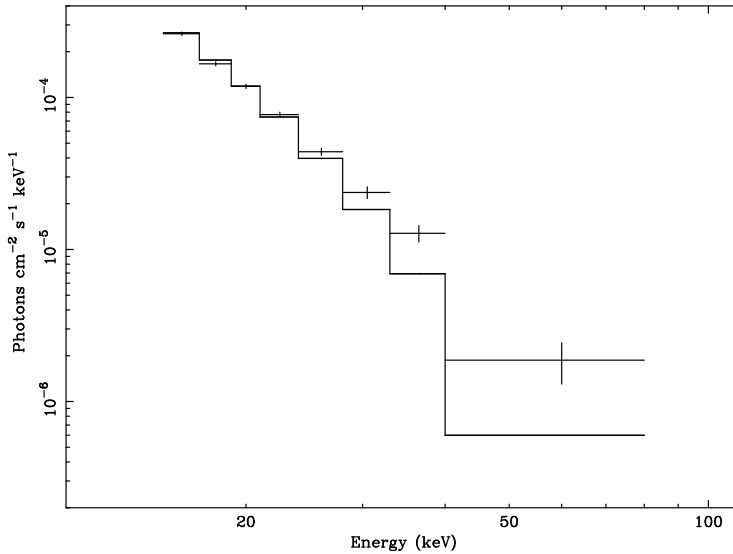


**Fig. 2** *BeppoSAX* spectrum of the Coma cluster obtained using the XAS software package (from Fusco-Femiano et al. 2007). Data are from PDS measurements (above 15 keV, with 68 % error bars); the line is a best-fit thermal model with  $kT = 8.11$  keV obtained previously from *Ginga* measurements (David et al. 1993).

the exact value of the temperature adopted in the analysis. Landi (2005) analysed a sample of 868 blank fields and found no difference in flux values when using either of the two offset pointings. However, Rossetti & Molendi (2007) could not investigate the reasons for the discrepancy between their blank sky measurements and those of Landi (2005) since the details of the latter work are not yet publicly available.

Flux confusion due to unidentified (and therefore unremoved) background AGN is particularly troublesome due to the relatively large FOV ( $1.3^\circ$ ) of the PDS. Although some of the integrated emission of distant AGN in the cluster field is removed in the rocking mode, there still is a residual signal due to AGN background fluctuations, and possibly also the presence of AGN in the cluster. This introduces a level of systematic uncertainty that was not specifically accounted for in most published PDS cluster analyses. Analysing 164 PDS blank-sky observations, Nevalainen et al. (2004) found a systematic difference in the background-subtracted fluxes when using only one of the two pointings available for the local background estimate in the standard rocking mode. The authors speculate that this might be due to either radiation entering the collimators from the side, screening of the instruments by the satellite, or the fact that the detector is looking at more/less radioactive parts of the satellite. These results are qualitatively similar to those of Rossetti & Molendi (2004), but are more pronounced by a factor of  $\sim 2$ . The difference in flux values when using either of the two offset pointings seems to be the reason for the different results obtained for the significance of the detection of NT emission in Coma. The issue remains unsettled and needs to be further explored.

Moreover, as we have pointed out, precise separation between the primary and secondary spectral components depends very much on the ability to do a simultaneous

**Table 2** NT emission parameters from *BeppoSAX* measurements and (deduced mean radio-and-X-determined field)  $B_{\text{rx}}$ 

Cluster	20 – 80 keV flux ( $10^{-12}$ erg s $^{-1}$ cm $^{-2}$ )	$\Gamma$	$B_{\text{rx}}$ ( $\mu\text{G}$ )	Reference
Coma <sup>a</sup>	$15 \pm 5$	?	0.2	Fusco-Femiano et al. (2004)
A 2256	$8.9^{+4.0}_{-3.6}$	$1.5^{+0.3}_{-1.2}$	0.05	Fusco-Femiano et al. (2000)
A 2199	$9.8 \pm 4.0$	$1.8 \pm 0.4$	?	Kaastra et al. (1999)
A 2319	$\leq 23$	?	$\geq 0.04$	Molendi et al. (1999)
A 3667 <sup>b</sup>	$\leq 6.4$	2.1	$\geq 0.4$	Fusco-Femiano et al. (2001)
A 754 <sup>c</sup>	$\sim 2$	?	0.1	Fusco-Femiano et al. (2003)
Centaurus <sup>d</sup>	$10.2 \pm 4.6$	$1.5^{+2.3}_{-1.3}$		Molendi et al. (2002)

All quoted errors are at the 90 % confidence level.

<sup>a</sup> According to Rosetti & Molendi (2007) proper accounting for uncertainties makes the detection insignificant.

<sup>b</sup> The emission from AGN FRL339 was not subtracted out.

<sup>c</sup> The measured flux is possibly from the radio galaxy 26W20.

<sup>d</sup> The measured flux is possibly due to an AGN.

fit to the parameters of both thermal and possibly NT emission. The search for a NT component with *BeppoSAX* suffered from lack of spectral overlap between the MECS and PDS instruments, and consequently the need to *adopt* a previously determined value of  $kT$ . Due to inherent differences between the *HEXTE* and *PDS* instruments, only a rough comparison between the respective results can be made. In this spirit it is apparent that the two estimates for the NT (20 – 80 keV) flux (Rephaeli & Gruber 2002; Fusco-Femiano et al. 2004) are in agreement (see Tables 1 & 2).

**A 2256:** Fusco-Femiano et al. (2005) analysed two separate PDS observations of the cluster for a total of  $\sim 430$  ks; they claimed a  $4.8\sigma$  detection of excess emission. Fitting this excess to a power-law yielded  $\Gamma = 1.5^{+0.3}_{-1.2}$  and a 20 – 80 keV flux of  $8.9 \times 10^{-12}$  erg cm $^{-2}$  s $^{-1}$ , which is essentially the same value deduced by Nevalainen et al. (2004). Use of the measured radio flux yielded  $B_{\text{rx}} \sim 0.05$   $\mu\text{G}$ , assuming that the NT emission they deduced originates in the radio relic located in the NW side of the cluster. We note that the flux deduced by Rephaeli & Gruber (2003) is about a factor of  $\sim 2$  lower than that of Fusco-Femiano et al. (2005), but given the large uncertainty in  $\Gamma$ , for which the former authors quote a relatively low value, this difference is not very significant.

**A 2199:** Analysis of MECS 8 – 10 keV measurements led Kaastra et al. (1999) to claim detection of a significant excess emission (over that of the best-fit thermal model). Fit of a power-law to the data yielded an index of  $1.81 \pm 0.25$ . They concluded that this emission originates in an outer region (beyond a 300 kpc central radial region), and that its relative strength (with respect to thermal emission) increases such that it dominates the 8 – 10 keV emission at  $\sim 1$  Mpc from the centre.

**A 3667:** A marginal detection (at a  $2.6\sigma$  significance) of excess 20 – 35 keV emission was reported by Fusco-Femiano et al. (2001). A power-law fit resulted in an index of  $\sim 2.1$ , from which an upper limit on NT 20 – 80 keV flux of  $6.4 \times 10^{-12}$  erg s $^{-1}$  cm $^{-2}$ , and a lower limit  $B_{\text{rx}} \simeq 0.4$   $\mu\text{G}$  were deduced. However, the authors did not consider the impact of the presence of the Seyfert 1 galaxy FRL 339 in the PDS FOV; emission from this galaxy is at a level comparable to that attributed to the NT component (Nevalainen et al. 2004). This would seem indeed the case, given the fact that analysis of *RXTE* measurements yielded only an upper limit on NT emission (Rephaeli & Gruber 2004).

**A 754:** Fusco-Femiano et al. (2003) reported the detection of excess emission above 45 keV at a  $3.2\sigma$  significance. They deduced a 10 – 40 keV flux of  $2 \times 10^{-12} \text{ erg s}^{-1} \text{ cm}^{-2}$  and  $B_{\text{rx}} \simeq 0.1 \mu\text{G}$ , but noted that the presumed NT emission could possibly be from the radio galaxy 26W20.

**Centaurus:** Molendi et al. (2002) detected a hard X-ray excess at the  $3.6\sigma$  level. The best-fit power-law model yielded an index of  $\Gamma = 1.5_{-0.8}^{+1.4}$ , and a 20 – 200 keV flux of  $2.2 \times 10^{-11} \text{ erg s}^{-1} \text{ cm}^{-2}$ , but they concluded that the emission may originate in a serendipitous AGN.

**A 2319:** No statistically significant power-law emission was detected in the analysis of a very short  $\sim 20$  ks (PDS) observation, resulting in an upper limit of  $2 \times 10^{-11} \text{ erg s}^{-1} \text{ cm}^{-2}$ , and a lower limit  $B_{\text{rx}} \sim 0.04 \mu\text{G}$  (Molendi et al. 1999). As discussed above, the much longer ( $\sim 160$  ks) *RXTE* observation led to a significant NT flux.

### 3.4.2 Statistical results from a cluster sample

An attempt to obtain some insight from co-added PDS data on a sample of 27 clusters was made by Nevalainen et al. (2004). A brief review of their results follows.

The problematic aspects of a statistical study of PDS data should first be summarised. As we have already noted, flux confusion due to unidentified AGN is of particular concern due to the relatively large PDS FOV. Nevalainen et al. (2004) used optical catalogues to identify Seyfert 1 galaxies, and BeppoSAX MECS or ROSAT PSPC data at their locations to estimate the AGN contribution in the PDS spectra. Clusters for which the estimated Seyfert 1 contribution was more than 15 % of the total signal were removed from the initial sample. Population synthesis modelling of the cosmic X-ray background (CXB) indicates that 80 % of the AGN need to be obscured to produce the CXB spectrum (Gilli et al. 1999), which is harder than the spectrum of unobscured AGN. Indeed, recent deep X-ray observations of blank fields (e.g., Hasinger et al. 2001) have discovered a population of absorbed point sources that outnumber the Seyfert 1 galaxies by a factor of  $\sim 4$ . These obscured AGN are seen through an absorbing torus (with  $N_{\text{H}} = 10^{22} - 10^{25} \text{ atoms cm}^{-2}$ ; Risaliti et al. 1999) which hides them in the soft X-ray band. Thus, a robust estimate for their contribution was not available. However, the spectral and spatial distribution of the NT emission (see below) argues against significant contamination due to obscured AGN in the final Nevalainen et al. (2004) sample.

The thermal emission of clusters in the sample was modelled by Nevalainen et al. (2004) based on results of published analyses of the emission measured by the BeppoSAX MECS and XMM-Newton EPIC instruments. Since the PDS has no spatial resolution, the flux observed in the central region was extrapolated to the full PDS FOV using the appropriate single (or double)  $\beta$  models, after account was made for vignetting. They extrapolated the thermal emission model to the 20 – 80 keV band and compared the prediction with the PDS data, thus estimating the NT emission. The comparison showed that in  $\sim 50$  % of the clusters the NT component was marginally detected at the  $2\sigma$  level. Most of the significant detections were found in clusters which show signs of recent merger activity. Specifically, when clusters were divided into ‘relaxed’ or ‘merger’ groups, it was determined that the mean 20 – 80 keV NT emission in the latter group ( $4.8 \times 10^{-2} \text{ counts s}^{-1}$ ) was  $\sim 10$  times higher than that of the ‘relaxed’ clusters (see Fig. 3). The level of systematic uncertainties due to background fluctuations is such that only the emission from clusters in the ‘merger’ group was found to be marginally significant (at  $\sim 2\sigma$ ). Assuming a power-law shape for this

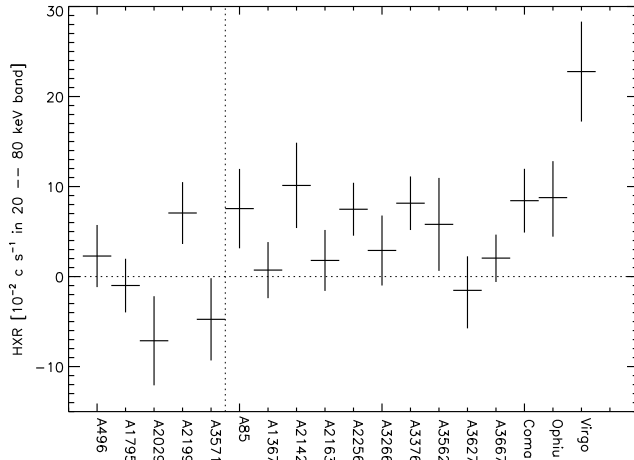


**Fig. 3** NT signal and  $1\sigma$  uncertainties in the PDS 20 – 80 keV band after subtraction of the contributions from the background, thermal emission, and AGN in the field, and accounting for uncertainties in these subtractions (Nevalainen et al. 2004). The dotted vertical line separates the relaxed clusters (left) from the rest (right).

excess with (photon) index of 2.0, it was deduced that the 20 – 80 keV luminosity per cluster is  $4 \times 10^{43} h_{70}^{-2} \text{ erg s}^{-1}$  (Nevalainen et al. 2004).

The residual emission of the individual clusters was too weak for meaningful spectral analysis; therefore, Nevalainen et al. (2004) co-added the data for the clusters, which amounted to a total of 560 ks. In order to obtain an estimate for the thermal contribution, the authors fitted data in the 12 – 20 keV band obtaining a best-fit temperature of  $\sim 8$  keV, consistent with the sample median. Extrapolating this model to the 20 – 80 keV band showed that there was indeed excess emission (see Fig. 4). A fit of the full 12 – 115 keV data to a thermal model resulted in a statistically unacceptable fit with an unrealistically high temperature of  $\sim 26$  keV.

A fit of the residual emission with a power-law model yielded a best-fit index  $\Gamma = 2.8_{-0.4}^{+0.3}$  at 90 % CL. Since a typical AGN index is  $\sim 1.8$ , appreciable AGN emission was ruled out at the 98 % CL. The high level of NT emission in the 12 – 20 keV band ( $\sim 50$  % of the total) is problematic, because in the central regions of the clusters in which NT emission was deduced, the MECS data typically allow the fractional contribution of such emission to be only a few percent. This seems to suggest that NT emission is extended with only a small fraction originating in the central region.

The indication from these statistical results for a connection between the cluster merger state and NT emission may be seen to support the scenario whereby electrons are accelerated by merger shocks. If so, the deduced power-law indices correspond to differential relativistic electron spectra with indices in the range  $\mu = 3.8 - 5.0$ . The implied radio synchrotron (energy) spectral indices  $\sim 1.4 - 2$ , are consistent with the observed range.

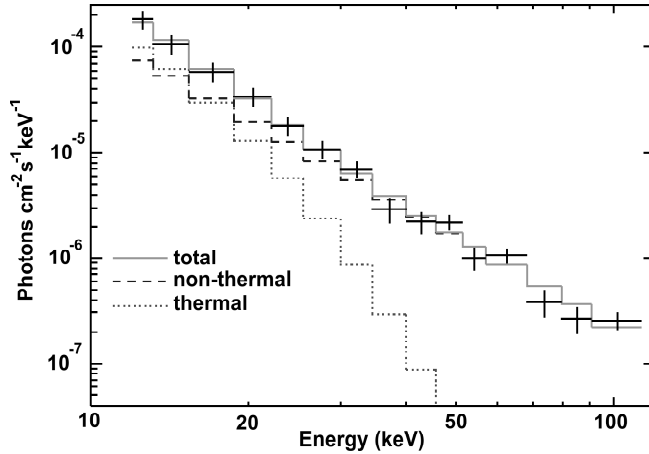


**Fig. 4** The combined PDS spectrum of all the clusters not significantly affected by AGN (Nevalainen et al. 2004). Lines show the unfolded model components while crosses show the data and  $1\sigma$  errors. The dotted line describes the thermal component, and the solid line shows the combined thermal and NT components. The dashed line indicates the best-fit power-law of  $\Gamma = 2.8$ .

### 3.5 Search for NT emission with *ASCA*

*ASCA* had a fairly good sensitivity and low background up to about 10 keV, clearly too low for observing cluster NT emission. But there could also be detectable NT emission in groups of galaxies, in which galaxy interactions occur at relatively high encounter rates, and given that gas temperatures in groups are typically about 2 keV or less, an attempt was made to look for NT emission with *ASCA*. The first reported detection of excess emission, at energies above 5 keV, was made for the group HCG 62 (Fukazawa et al. 2001). The luminosity of the excess component was  $\sim 4 \times 10^{41}$  erg  $s^{-1}$ , which was estimated to be some 20 times higher than the contribution of discrete X-ray sources. The hard excess was spatially extended to about  $10'$  from the centre. Since the spectrum was too hard to be interpreted as thermal emission from the intra-group gas, a NT origin was thought to be more likely. A recent analysis of *Suzaku* XIS and HXD (see below) measurements of HCG 62 resulted only in an upper limit on NT emission (Tokoi et al. 2007), but at a level which does not exclude the *ASCA* result.

Nakazawa et al. (2007) carried out a search for NT emission from 18 groups of galaxies observed with *ASCA*, including HCG 62. They fitted the spectra below 2.5 keV with 2 temperature thermal (MEKAL) models and compared the data in the 4–8 keV band with the extrapolated thermal spectra. Excess fluxes are shown in Fig. 5 in terms of statistical significance. HCG 62 and RGH 80 show excess emission at  $> 2\sigma$  CL, with excess emission thought to be likely also in NGC 1399. The residual spectra could be fitted either with a thermal model with  $kT \geq 3$  keV or a power-law model with photon index fixed at 2. The 2–10 keV luminosity of the excess component is 10–30 % of the thermal emission and 4–100 times stronger than the contribution from discrete X-ray sources. They concluded that both thermal and NT origins are acceptable from a statistical point of view.



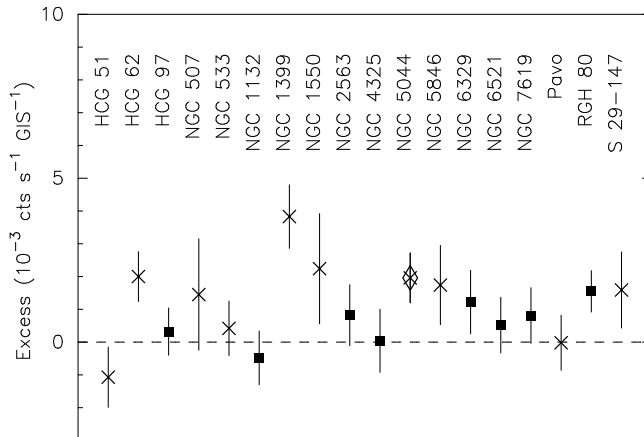


**Fig. 5** ASCA measurement of excess emission in a sample of 18 groups of galaxies. The count rate in the 4 – 8 keV band is shown by the residual over the thermal model determined in the energy range below 2.5 keV. Squares denote groups for which the soft-band spectrum was fitted with single temperature model, while in the systems shown by stars two-temperature models were required. Error bars include statistical and systematic  $1\sigma$  uncertainties. A thermal fit to the NGC 5044 spectrum, indicated with a diamond, was considered to be unacceptable. Adapted from Nakazawa et al. (2007).

### 3.6 Search for NT emission with *Suzaku*

*Suzaku*, the 5th Japanese X-ray satellite launched in July 2005, carries hard X-ray detectors (HXD) along with the X-ray CCD instrument (XIS). The combined energy range is from 0.3 keV up to about 600 keV, and a wide-band coverage of X-ray and  $\gamma$ -ray sources is possible. The HXD system consists of 16 units of well-type phoswich detectors, surrounded by anti-coincidence shield scintillators (Takahashi et al. 2007; Kokubun et al. 2007). The well-type detector consists of a long active collimator made of BGO (a Bismuth-Germanium Oxyde), and the bottom of the well is equipped with Si PIN detectors and a GSO (a Gadolinium-Silicon Oxyde) scintillator. The PIN is 2 mm thick and sensitive from 8 keV to 50 keV; the GSO covers the 50 – 600 keV band. Typical effective areas are  $160 \text{ cm}^2$  at 10 keV (PIN), and  $330 \text{ cm}^2$  at 100 keV (GSO). The FOV is  $34' \times 34'$  FWHM below 100 keV, limited by a phosphor bronze fine collimator installed in the well. At higher energies, the FOV becomes wider, up to  $4.5^\circ \times 4.5^\circ$ . The PIN detectors are cooled to  $-20^\circ\text{C}$  by a thermal radiator connected with heat pipes.

The background level is very low for the PIN detector, since it has no accumulated effect of radio-activation in orbit. The measured background level in orbit is indeed lower than the level of the PDS (on BeppoSAX) by a factor of about 3, even though *Suzaku*'s inclined orbit makes it more susceptible to the intense X-rays during passage through the radiation belt. This and the HXD narrow FOV make it the most sensitive instrument in the 10 – 60 keV band, among all previously flown hard X-ray detectors.

About 30 clusters have already been observed (as of April 2007) with *Suzaku*, including several for which the primary purpose is a search for NT emission. Meaningful constraints on NT emission were obtained for rather low temperature clusters. Most extensively observed is A 3376; these observations are described in some detail.

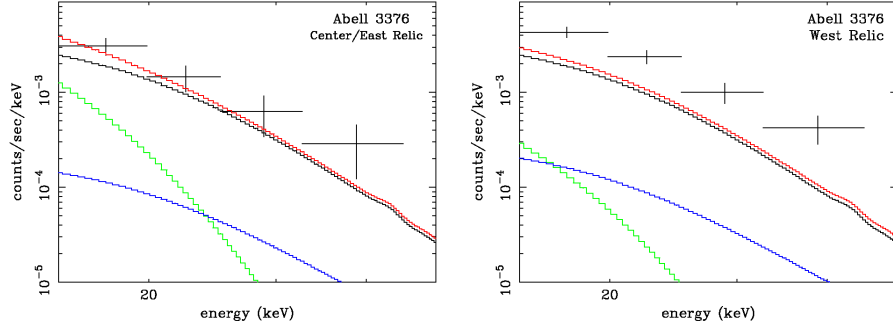


**Fig. 6** Background subtracted spectra of A 3376 with the *Suzaku* HXD PIN detector (Kawano et al. 2007). Left panel is for the region including the centre and the east relic; the right panel is for the west relic. Upward along the left-hand ordinate, the four solid curves show estimated flux due to point-sources, cluster thermal emission, cosmic X-ray background contribution, and their sum, respectively.

**A 3376:** This nearby ( $z = 0.046$ ) merging cluster has an IC gas temperature of  $\sim 4$  keV. The relatively low temperature motivated the selection of the cluster as the prime target for observations with the PIN detectors. The cluster is noted by two large radio relics, probably expanding over a Mpc scale in the east and west boundaries of the thermal emission. BeppoSAX observations resulted in a  $2.7\sigma$  detection of a NT component. The *Suzaku* observations were carried out during two separate pointings in October and November 2005. The first  $\sim 90$  ks observation covered the central region which includes the east relic, and the second  $\sim 103$  ks was centred on the west relic region.

The background properties have been investigated by Kawano et al. (2007) and applied to the A 3376 data. Background data, i.e. data taken when the satellite was pointing to the dark Earth, were sorted by position of the satellite in Earth coordinates. This basically performs sorting with the cosmic-ray cut-off rigidity which is known to correlate well with the non X-ray background. Since passage through the radiation belt leaves enhanced emission afterward, the data in each Earth position were further divided into northward and southward satellite movements. The long-term trend of the background variation was also included in the estimation. Comparison with the predicted background rate and the observed dark Earth data indicates that this method gives 3.5 % ( $1\sigma$ ) error.

This method was applied to the observed data in the energy range 15–50 keV. Thermal cluster emission, estimated from the XIS measurements, CXB and point source contributions need to be subtracted. As shown in Fig. 6, the HXD PIN spectrum for the west relic suggests some level of excess emission. Including fluctuations of all these components, the flux of the west relic in the 15–50 keV band is  $(6.3 \pm 1.8 \pm 6.2) \times 10^{-12}$  erg cm $^{-2}$  s $^{-1}$ , where the errors are statistical and systematic, respectively. Most of the systematic error, about 85 %, is non-CXB; thus, further improvement in the background estimation is necessary in order to better determine the level of excess emission. The implied upper limit,  $1.4 \times 10^{-11}$  erg cm $^{-2}$  s $^{-1}$ , is consistent with the limit obtained from the *RXTE* measurements, and about 20 % lower than the level reported from the *BeppoSAX* observation.

The west-relic region was jointly observed with the XIS instrument, and Kawano et al. also constrained the possible power-law flux based on the spectral fit. The obtained upper limit in the 4 – 8 keV region is extrapolated to 15 – 50 keV assuming a photon index of 1.8 with no scaling with the FOV, and it corresponds to about 20 % of the hard X-ray upper limit. Of course, it is quite possible that the true NT flux is less than  $3 \times 10^{-12} \text{ erg cm}^{-2} \text{ s}^{-1}$  in the 15 – 50 keV band; however, if the emission is spatially extended then the XIS constraint still allows a hard flux of  $2.4 \times 10^{-11} \text{ erg cm}^{-2} \text{ s}^{-1}$  over the PIN field of view. Thus, an extended hard X-ray emission (larger than  $0.5^\circ$ ) remains a possibility. Using the 1.4 GHz measurement of the west relic, Kawano et al. deduced a lower limit  $B_{\text{rx}} > 0.1 \mu\text{G}$ .

**A 1060 and the Centaurus cluster:** These clusters are both relaxed nearby systems with  $kT \sim 3.5 \text{ keV}$ ; A 1060 is non-cD cluster, while the Centaurus cluster is dominated by a cD galaxy. The clusters were well studied by Kitaguchi et al. (2007). The observed data for the A 1060 and Centaurus cluster by the PIN instrument were accumulated for 28 and 26 ks, respectively. The latter authors applied the standard non-CXB subtraction and found that the blank-sky data yielded a fluctuation of 3 – 5 % ( $1\sigma$ ) in the energy range 10 – 50 keV. When the non-CXB flux was subtracted from the data, the data for both clusters showed agreement with the CXB above 20 keV; the A 1060 data even showed a deficit of the counts. In the energy range 10 – 20 keV, there remained an excess flux over the CXB level for both clusters. The flux was 4 or 8 times stronger than the CXB level for A 1060 and Centaurus, respectively. The cluster thermal emission was measured with ASCA, which had a wider FOV than the PIN, and the measured temperatures were 3.3 and 3.8 keV for the two clusters. These spectra with the intensity consistent with the ASCA measurement were compared with the PIN residual component. They found that the thermal emission can explain the PIN data quite well for both clusters, so only upper limits were derived on the NT emission.

### 3.7 INTEGRAL observation of the Coma cluster

A large fully coded field of view ( $8^\circ \times 8^\circ$ ), and good imaging capabilities with a PSF of  $12'$  FWHM, make it possible to construct hard X-ray cluster images below 300 keV with the IBIS/ISGRI coded mask instrument (Ubertini et al. 2003; Lebrun et al. 2003) aboard the *International Gamma-Ray Astrophysics Laboratory* (INTEGRAL, Winkler et al. 2003). Renaud et al. (2006) reported the analysis of a  $\sim 500$  ks observation of the Coma cluster with IBIS/ISGRI. The cluster was detected at a significance  $\sim 10\sigma$  CL in the 18 – 30 keV energy band. The ISGRI image shows extended emission structure globally similar to that is seen by XMM-Newton below 10 keV (e.g. Arnaud et al. 2001; Neumann et al. 2003). In Fig. 7 we present two images of the Coma field in the 18 – 30 keV (left panel) and 30 – 50 keV (right panel) energy bands processed with the OSA-5 software, following a procedure similar to that described in Renaud et al. (2006), but for a longer (accumulated) ISGRI exposure of  $\sim 940$  ks (‘good time’). The detected flux in the 18 – 30 keV band is consistent with the extrapolation of the flux measured by XMM-Newton below 10 keV assuming a model of a thin thermal plasma model with  $kT = 8 \text{ keV}$  (see Renaud et al. 2006; Eckert et al. 2007); no statistically significant flux is seen in the higher energy band. From the observed images it appears that in order to detect or meaningfully constrain with INTEGRAL the presence of a NT X-ray component reported in RXTE and BeppoSAX observations of Coma, an integration time longer by a factor of  $\sim 2 - 3$  would be required.

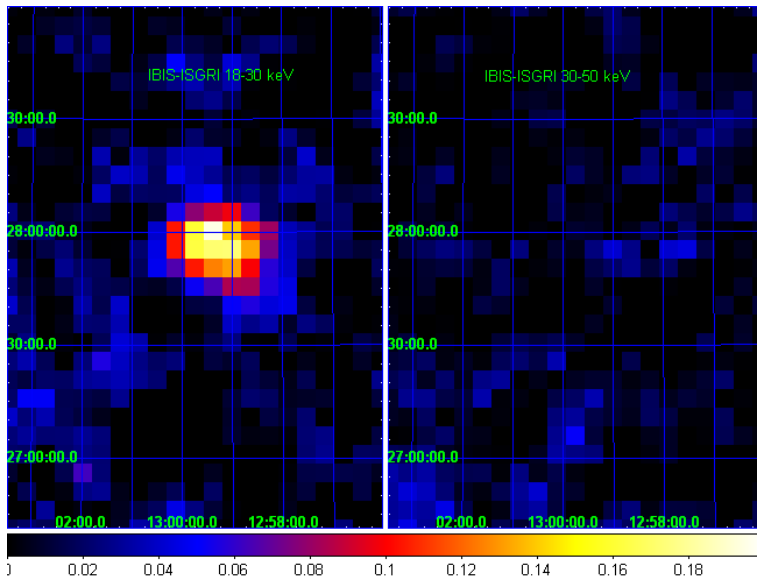


**Fig. 7** Hard X-ray images of the Coma cluster from a 940 ks *IBIS-ISGRI* observation. The left and right panels show the *ISGRI* mosaics in the 18 – 30 keV, and 30 – 50 keV bands, respectively.

### 3.8 Limits on cluster $\gamma$ -ray emission

The relatively steep power-law shape of cluster NT emission (which is most precisely measured in the radio) directly implies that the detection of  $\gamma$ -ray emission from even nearby clusters will be very challenging. To estimate the predicted level of emission, consider the Coma cluster as an example; assuming no change in the relativistic electron power-law index, and the deduced 20 – 80 keV flux level (in Table 1), the cumulative flux at  $\epsilon \geq 100$  MeV is  $\sim 6 \times 10^{-9} \text{ cm}^{-2} \text{ s}^{-1}$ . Although substantially uncertain, flux at this level is close to the projected *GLAST* sensitivity threshold for an exposure time of 1 yr for the all sky survey. The flux will be well below this level if the electron spectrum steepens even modestly at energies above the range deduced from radio measurements. Note that  $\gamma$ -ray emission could also have hadronic origin (from  $\pi^0$  decay, following proton-proton interactions), but only very rough limits can be placed on this emission (e.g., Dermer & Rephaeli 1988).

A statistical upper limit on  $\gamma$ -ray emission from clusters was obtained by Reimer et al. (2003) from analysis of *EGRET* measurements. The emission in fields centred at 58 clusters observed between 1991 and 2000 was analysed. A co-added mean flux level was determined after accounting for the diffuse background contribution. The resulting upper  $2\sigma$  limit on the mean cluster flux above (photon) energy of  $\epsilon \geq 100$  MeV was found to be  $6 \times 10^{-9} \text{ cm}^{-2} \text{ s}^{-1}$ . Interestingly, this level is at the level predicted for Coma based on direct extrapolation of the deduced 20 – 80 keV flux. This *EGRET* upper limit was used by Bykov et al. (2000) and Petrosian (2001) to constrain models of hard X-ray emission components of leptonic origin; similarly Blasi & Colafrancesco (1999) used it to constrain the energetic proton energy density in IC space.

---

## 4 Discussion

It has been known all along that definite detection of NT X-ray emission in clusters is a challenging task. This is due to several factors, major among which are its intrinsically weak level - swamped as it is by the intense primary thermal emission - and the difficult to achieve requisite high sensitivity and low detector background in the 10 – 100 keV band. As has been emphasised, results of the search are not unequivocal, even for Coma and A 2256 for which detection (by *RXTE* and *BeppoSAX*) was claimed to be at moderately high level of statistical significance. This is mainly due to source confusion and a complete lack of spatial information. The search should continue (with *Suzaku* and future satellites), spurred by its sound physical basis - the ubiquity of the CMB, and the observed radio synchrotron emission from relativistic electrons.

The expected level of NT emission of Compton origin depends steeply on the mean magnetic field strength in the central cluster region. Clearly, if this is typically a fraction of a  $\mu\text{G}$ , as has been deduced in the analyses described in the previous section, then prospects for more definite detection of NT emission - perhaps already with deep *Suzaku* measurements - are indeed good. However, significantly higher  $B_{\text{fr}}$  values - a few  $\mu\text{G}$  - are deduced from FR measurements; had these been meaningful estimates of the *volume-averaged* field strength, then definite detection of NT emission would have been seriously questioned.

As we have noted already (in Sect. 2.2), the apparent discrepancy between deduced values of  $B_{\text{rx}}$  and  $B_{\text{fr}}$  has been investigated at some length. These two field measures are quite different; the former is essentially a volume average of the relativistic electron density and (roughly) the square of the field, the latter is an average along the line of sight of the product of the field and gas density. All these quantities vary considerably across the cluster; in addition, the field is very likely tangled, with a wide range of coherence scales which can only be roughly estimated. These make the determination of the field by both methods considerably uncertain. Thus, the unsatisfactory observational status (stemming mainly from lack of spatial information) and the intrinsic difference between  $B_{\text{rx}}$  and  $B_{\text{fr}}$ , do not allow a simple comparison of these quantities. Even if the large observational and systematic uncertainties, the different spatial dependences of the fields, relativistic electron density, and thermal electron density, already imply that  $B_{\text{rx}}$  and  $B_{\text{fr}}$  will in general be quite different. This was specifically shown by Goldshmidt & Rephaeli (1993) in the context of reasonable assumptions for the field morphology, and the known range of IC gas density profiles. They concluded that  $B_{\text{rx}}$  is indeed generally smaller than  $B_{\text{fr}}$ . The implication is that prospects for detection of NT emission should not be based on the relatively high deduced values of  $B_{\text{fr}}$ .

In conclusion, *RXTE* and *BeppoSAX* measurements have yielded appreciable evidence for power-law X-ray emission in four clusters. These results motivate further measurements and theoretical studies of NT phenomena on cluster and cosmological scales.

**Acknowledgements** The authors thank ISSI (Bern) for support of the team “Non-virialized X-ray components in clusters of galaxies”.

---

**References**

- Arnaud, M., Aghanim, N., Gastaud, R., et al., 2001, *A&A*, 365, L67
- Blasi, P., Colafrancesco, S., 1999, *Astropar. Phys.*, 122, 169
- Bykov, A.M., Bloemen, H., & Uvarov Yu.A., 2000, *A&A*, 362, 886
- Carilli, C.L., Taylor, G.B., 2002, *ARAA*, 40, 319
- Clarke, T.E., Kronberg, P.P., & Böhringer, H., 2001, *ApJ*, 547, L111
- Clarke, T.E., *J. Kor. Astr. Soc.*, 37, 337
- David, L.P., Slyz, A., Jones, C., et al., 1993, *ApJ*, 412, 479
- Dennison, B., 1980, *ApJ*, 239, L93
- Dermer, C.D. & Rephaeli, Y., 1988, *ApJ*, 329, 687
- Dolag, K., Schindler, S., Govoni, F., & Feretti, L., 1999, *A&A*, 378, 777
- Dreher, J.W., Carilli, C.L., & Perley, R.A., 1987, *ApJ*, 316, 611
- Durret, F., Kaastra, J., Nevalainen, J., Ohashi, T. & Werner, N., 2008, SSR, in press
- Eckert, D., Neronov, A., Courvoisier, T. J.-L., & Produit, N., 2007, *A&A*, 470, 835
- Enßlin, T.A., Vogt, C., Clarke, T.E., & Taylor, G.B., 2003, *ApJ*, 597, 870
- Ferrari, C., Govoni, F., Schindler, S., Bykov, A.M., & Rephaeli, Y., 2008, SSR, in press
- Feretti, L., Dallacasa, D., Govoni, F., et al., 1999, *A&A*, 344, 472
- Fukazawa, Y., Nakazawa, K., Isobe, N., et al., 2001, *ApJ*, 546, L87
- Fusco-Femiano, R., Dal Fiume, D., Feretti, L., et al., 1999, *ApJ*, 513, L21
- Fusco-Femiano, R., Dal Fiume, D., De Grandi, S., et al., 2000, *ApJ*, 534, L7
- Fusco-Femiano, R., Dal Fiume, D., Orlandini, M., et al., 2001, *ApJ*, 552, L97
- Fusco-Femiano, R., Orlandini, M., de Grandi, S., et al., 2003, *A&A*, 398, 441
- Fusco-Femiano, R., Orlandini, M., Brunetti, G., et al., 2004, *ApJ*, 602, L73
- Fusco-Femiano, R., Landi, R., Orlandini, M., 2005, *ApJ*, 624, L69
- Fusco-Femiano, R., Landi, R., & Orlandini, M., 2007, *ApJ*, 654, L9
- Gilli, R., Risaliti, G., & Salvati, M., 1999, *A&A*, 347, 424
- Giovannini, G., Feretti, L., Venturi, T., Kim, K.-T., & Kronberg, P.P., 1993, *ApJ*, 406, 399
- Giovannini, G., Tordi, M., & Feretti, L., 1999, *New Astron.*, 4, 141
- Giovannini, G., & Feretti, L., 2000, *New Astron.*, 5, 335
- Giovannini, G., Feretti, L., Govoni, F., Murgia, M., & Pizzo, R., 2006, *AN*, 327, 563
- Goldshmidt, O., & Rephaeli, Y., 1993, *ApJ*, 411, 518
- Gruber, D.E., & Rephaeli, Y., 2002, *ApJ*, 565, 877
- Govoni, F., & Feretti, L., 2004, *Int. J. Mod. Phys. D*, 13, 1549
- Hasinger, G., Altieri, B., Arnaud, M., et al., 2001, *A&A*, 365, L45
- Henriksen, M., 1999, *ApJ*, 511, 666
- Henriksen, M., & Mushotzky, R., 2001, *ApJ*, 553, 84
- Kaastra, J.S., Bleeker, J.A.M. & Mewe, R., 1998, *Nuc. Phys. B*, 69, 567
- Kaastra J.S., Lieu, R., Mittaz, J., et al., 1999, *ApJ*, 519, L119
- Kawano, N., Nakazawa, K., Fukazawa, Y., et al., 2007, in proc. of ‘The Extreme Universe in the *Suzaku* Era’, conf. CD, in press
- Kim, K.-T., Kronberg, P.P., & Tribble, P.C., 1991, *ApJ*, 379, 80
- Kitaguchi, T., Makishima, K., Nakazawa, K., et al., 2007, in proc. of ‘The Extreme Universe in the *Suzaku* Era’, conf. CD, in press
- Kokubun, M., Makishima, K., Takahashi, T., et al., 2007, *PASJ*, 59, 53
- Landi, R., 2005, Ph.D. thesis, Bologna University
- Lebrun, F., Leray, J.P., Lavocat, P., et al., 2003, *A&A*, 411, L141
- Mohr, J. J., Mathiesen, B., & Evrard, A. E. 1999, *ApJ*, 517, 627

- 
- Molendi, S., de Grandi, S., Fusco-Femiano, R., et al., 1999, *ApJ*, 525, L73  
Molendi, S., De Grandi, S., & Guainazzi, M., 2002, *A&A*, 392, 13  
Murgia, M., Govoni, F., Feretti, L., et al., 2004, *A&A*, 424, 429  
Nakazawa, K., Makishima, K., & Fukazawa, Y., 2007, *PASJ*, 59, 167  
Neumann, D. M., Lumb, D. H., Pratt, G.W., & Briel, U. G., 2003, *A&A*, 400, 811  
Nevalainen, J., Oosterbroek, T., Bonamente, M., & Colafrancesco, S., 2004, *ApJ*, 608, 166  
Newman, W.I., Newman, A.L., & Rephaeli, Y., 2002, *ApJ*, 575, 755  
Petrosian, V., 2001, *ApJ*, 557, 560  
Petrosian, V., Madejski, G., & Luli, K., 2006, *ApJ*, 652, 948  
Petrosian, V., Bykov, A.M., & Rephaeli, Y., 2008, *SSR*, in press  
Petrosian, V., & Bykov, A.M., 2008, *SSR*, in press  
Reimer, O., Pohl, M., Sreekumar, P., & Mattox, J.R., 2003, *ApJ*, 588, 155  
Renaud, M., Belanger, G., Paul, J., Lebrun, F. & Terrier, R., 2006, *A&A*, 453, L5  
Rephaeli, Y., 1977, *ApJ*, 212, 608  
Rephaeli, Y., 1979, *ApJ*, 227, 364  
Rephaeli, Y., 1987, *MNRAS*, 225, 851  
Rephaeli, Y., 2001, in *Proc. of Heidelberg Int. Symp.*, AIP Conf. Ser., 558, 427  
Rephaeli, Y., & Gruber, D.E., 1988, *ApJ*, 333, 133  
Rephaeli, Y., & Gruber, D.E., 2002, *ApJ*, 579, 587  
Rephaeli, Y., & Gruber, D.E., 2003, *ApJ*, 595, 137  
Rephaeli, Y., & Gruber, D.E., 2004, *ApJ*, 606, 825  
Rephaeli, Y., Gruber, D., & Rothschild, R., 1987, *ApJ*, 320, 139  
Rephaeli, Y., Gruber, D., & Ulmer, M., 1994, *ApJ*, 429, 554  
Rephaeli, Y., Gruber, D., & Blanco, P., 1999, *ApJ*, 511, L21  
Rephaeli, Y., Gruber, D.E., & Arieli, Y., 2006, *ApJ*, 649, 673  
Rephaeli, Y., & Silk, J., 1995, *ApJ*, 442, 91  
Rossetti, M., & Molendi, S., 2004, *A&A*, 414, 41  
Rossetti, M., & Molendi, S., 2007, electronic preprint only, astro-ph/0702417  
Risaliti, G., Maiolino, R., & Salvati, M., 1999, *ApJ*, 522, 157  
Rudnick, L., & Blundell, K., 2003, *ApJ*, 588, 143  
Sanders, J.S., & Fabian, A.C., 2007, *MNRAS*, 381, 1381  
Sarazin, C.L., 1999, *ApJ*, 520, 529  
Seeger, C.L., Westerhout, G., & Conway, R.G., 1957, *ApJ*, 126, 585  
Simionescu, A., Werner, N., Finoguenov, A., Böhringer, H. & Brüggén, M., 2007, *A&A*, submitted (astro-ph/0709.4499)  
Takahashi, T., Abe, K., Endo, M., et al., 2007, *PASJ*, 59, 35  
Taylor, G.B., & Perley, R.A., 1993, *ApJ*, 416, 554  
Thierbach, M., Klein, U., & Wielebinski, R., 2003, *A&A*, 397, 53  
Tokoi, K., Sato, K., Ishisaki, Y., et al., 2007, *PASJ*, vol. 60, in press (astro-ph/0711.1454)  
Ubertini, P., Lebrun, F., Di Cocco, G. et al., 2003, *A&A*, 411, L131  
Valinia, A., Henriksen, M., Loewenstein, M., et al., 1999, *ApJ*, 515, 42  
Vogt, C., Enßlin, T.A., 2003, *A&A*, 412, 373  
Willson, M.A.G., 1970, *MNRAS*, 151, 1  
Winkler, C., Courvoisier, T., Di Cocco, G., et al., 2003, *A&A*, 411, L1